HHS Public Access

Author manuscript

J Immunol. Author manuscript; available in PMC 2020 February 01.

Published in final edited form as:

J Immunol. 2019 February 01; 202(3): 899–911. doi:10.4049/jimmunol.1800712.

IRAK-M associates with susceptibility to adult-onset asthma and promotes chronic airway inflammation

Yi Liu[#,†,*], **Mingqiang Zhang**[#,*], **Lili Lou**[#], **Lun Li**[#], **Youming Zhang**[‡], **Wei Chen**[§], **Weixun Zhou**[§§], **Yan Bai**[¶¶], and **Jinming Gao**[#]

[#]Department of Respiratory Diseases, Peking Union Medical College Hospital, Chinese Academy of Medical Sciences & Peking Union Medical College, Beijing 100730, China

[§]Department of Cardiology, Peking Union Medical College Hospital, Chinese Academy of Medical Sciences & Peking Union Medical College, Beijing 100730, China

[§§]Department of Pathology, Peking Union Medical College Hospital, Chinese Academy of Medical Sciences & Peking Union Medical College, Beijing 100730, China

[†]Department of Respiratory Medicine, Civil Aviation General Hospital, Beijing, 100123, China

[‡]Genomics Medicine Section, National Heart and Lung Institute, Imperial College London, London, SW3 6LY, UK

[¶¶]Division of Pulmonary and Critical Care Medicine, Department of Internal Medicine, Brigham and Women's Hospital, Harvard Medical School, Boston, Massachusetts

Abstract

IL-1 receptor-associated kinase (IRAK) – M regulates lung immunity during asthmatic airway inflammation. However, the regulatory effect of IRAK-M differs when airway inflammation persists. A positive association between IRAK-M polymorphisms with childhood asthma has been reported. In this study, we investigated the role of IRAK-M in the susceptibility to adult-onset asthma and in chronic airway inflammation using an animal model. Through genetic analysis of IRAK-M polymorphisms in a cohort of adult-onset asthma patients of Chinese Han ethnicity, we identified two IRAK-M SNPs, rs1624395 and rs1370128, genetically associated with adult-onset asthma. Functionally, the top-associated rs1624395 with an enhanced affinity to the transcription factor C-Jun was associated with a higher expression of IRAK-M mRNA in blood monocytes. In contrast to the protective effect of IRAK-M in acute asthmatic inflammation, we found a provoking impact of IRAK-M on chronic asthmatic inflammation. Following chronic OVA

Correspondence to: Jinming Gao, M.D., Professor of Pulmonary Medicine, Department of Respiratory Diseases, Peking Union Medical College Hospital, #1 Shuaifuyuan, Dongcheng District, Beijing 100730, China., gjinming@yahoo.com, OR gaojim@pumch.cn, Tel: 861069155049, Fax: 861065124875.

[*]These authors equally contributed to this work.

Authors' contributions:

Y. L., M.Z., and L. L. performed the experiments; L.L. handled experimental animals; W.C. facilitated the experiments; W.Z. performed the pathological evaluations; Y.B. reviewed the experimental data and edited the manuscript for important intellectual contents; Y.Z. designed the experiments, reviewed the experimental data and edited the manuscript for important intellectual contents; J.G. designed and supervised this study, interpreted the experimental findings, and drafted the manuscript.

All authors were involved in experimental design, data interpretation, and manuscript preparation. All authors have read and approved the final version of this manuscript.

Conflict of interest statement

The authors declare that they have no conflict interest.

stimulation, IRAK-M knock-out (KO) mice presented with significantly less inflammatory cells, a lower Th2 cytokine level, a higher IFNγ concentration and increased percentage of Th1 cells in the lung tissue than wild-type (WT) mice. Moreover, lung dendritic cells (DC) from OVA-treated IRAK-M KO mice expressed a higher percentage of costimulatory molecules PD-L1 and PD-L2. Mechanistically, in vitro toll-like receptor ligation led to a greater IFNγ production by IRAK-M KO DCs than WT DCs. These findings demonstrated a distinctive role of IRAK-M in maintaining chronic Th2 airway inflammation via inhibiting the DC-mediated Th1 activation, and indicated a complex role for IRAK-M in the initiation and progression of experimental allergic asthma.

Keywords

asthma; IRAK-M; single nucleotide polymorphism; airway inflammation

Introduction

Asthma is a heterogeneous disease characterized by chronic airway inflammation and airway remodeling (1, 2), affecting patients of all ages (3, 4). Genome-wide association studies (GWAS) and positional cloning have identified multiple single nucleotide polymorphisms (SNP) of several asthma-associated genes expressing in airway epithelium, illustrating the critical role of the respiratory epithelial barrier in the pathogenesis of asthma (5, 6). Epithelium, in conjunction with type 2 innate lymphoid cells, dendritic cells, macrophages, and other cell types, constitutes an innate immune network in the airway. Activation of this immune network regulates the Th2/Th17 dominant adaptive immune response (7). A predisposition to asthma was shown to be related to the impaired host innate immunity (8). Moreover, GWAS reveals that the locus of IL-1 receptor-associated kinase (IRAK-M) gene on human chromosome 12q14.2 is one of the most consistently replicated regions linked to asthma or asthma-related traits in the diverse populations (9, 10). A positive association between IRAK-M SNPs and the early-onset asthma was reported in an Italian population (11). However, genetic studies on IRAK-M SNPs in asthma or atopy have yielded inconsistent results in children and adult patients in different populations (12–14). In addition to asthma, several IRAK-M SNPs have been implicated in other acute inflammatory diseases, such as acute lung injury (15).

IRAK-M, primarily expressed by dendritic cells (DC), macrophages, and airway epithelium, is an intracellular negative regulator of Toll-like receptors (TLRs) that regulates the innate immune homeostasis (11, 16). Evolving evidence has shown IRAK-M also participates the asthmatic immune responses. For instance, the expression of IRAK-M was upregulated in peripheral blood leukocytes in asthmatic children (8), and high mRNA expression of IRAK-M in sputum was a marker for frequent exacerbations of asthma (17). A unique feature of IRAK-M mediated regulation is that it varies in a disease stage-dependent manner (18). Accumulating evidence from us and others indicates that IRAK-M may exert contradictory roles, inhibitory or activating, in inflammatory and immune responses, depending on the duration of stimulation and the kind of stimuli. In our previous study using animal model, we demonstrated that IRAK-M knockout (KO) enhanced the acute airway inflammation to 3-day cigarette smoking, but attenuated the chronic inflammatory responses to 7-week

cigarette smoking, via differentially modulating the function of Treg, Th17, DCs, and macrophages (19). Similarly, others have demonstrated IRAK-M KO reduced the acute inflammatory responses to a noninfectious injury and subsequent fibrosis (20, 21). By contrast, overexpression of airway epithelial IRAK-M by IL-13 stimulation impaired the innate immunity and increased susceptibility to respiratory infection (22, 23). In particular, we have studied the regulatory effect of IRAK-M on the asthmatic airway inflammation utilizing the acute ovalbumin (OVA) mouse model and found that IRAK-M ablation exacerbated airway inflammation by enhancing Th2 and Th17 differentiation (24). These results support the multifactorial roles of IRAK-M signaling in modulating inflammatory responses (25). However, the impact of IRAK-M on chronic asthmatic inflammation remains unclear.

To fill in the knowledge gaps, in the present study, we assessed the role of IRAK-M in adult-onset asthma and the development of chronic asthmatic inflammation. First, using samples from a hospital-based asthma cohort with Chinese Han ethnicity, we explored the genetic association between IRAK-M SNPs and human adult-onset asthma and the functionalities of susceptible IRAK-M SNP. Next, utilizing a chronic OVA mouse model, we investigated the regulation of IRKA-M expression following repeated allergen exposure and the influence of IRAK-M loss on the chronic allergic inflammation and airway remodeling.

Materials and Methods

Participants

There were a total of 1348 subjects with Han ethnicity from the Northern region of China enrolled in this study. Six hundred and seventy nine patients with adult-onset asthma were recruited from two medical centers. Adult-onset asthma was defined as previously described (26). The asthma patients, who had their first symptoms at the age of 18 years or older, were fully characterized by clinical presentation, functional status, and inflammatory markers. Asthma patients with forced expiratory volume in the first second (FEV1) ≥ 70% of predicted underwent the methacholine (Mch) challenge test. Patients whose FEV1 was less than 70% of predicted underwent an airway reversibility test by β2 agonist. Six hundred and sixty nine age- and ethnicity-matched controls were selected from non-asthmatic, non-atopic, healthy individuals with normal lung function. All participants were unrelated. Detailed characteristics of these individuals were listed in Table 1.

The study protocols were approved by the Ethic Committee for Human Research of Peking Union Medical College Hospital (S-767) and Beijing Aviation General Hospital (MHZYY 2014–05–01) and all subjects gave informed written consent.

Genotyping

Genomic DNA from peripheral blood leukocytes was extracted by standard protocols. A total of 9 markers were genotyped. SNPs were genotyped using SNaPshot. The primers for PCR amplification and extension of IRAK-M gene are listed in Supplemental Tables 1 and 2. The PCR products were sequenced on an ABI 3730XL DNA Analyzer (Applied Biosystems) and analyzed using the GeneMapper 4 software.

The genotyping efficiency for IRAK-M SNPs was greater 95%. Minor allele frequency was > 5%, All SNPs tested were in Hardy–Weinberg equilibrium (p cutoff-value =0.05) in asthma cases and controls.

Quantitative RT-PCR (qRT-PCR) analysis for mRNA expression of IRAK-M in circulating monocytes in asthmatics

Total RNA was extracted from peripheral blood monocytes (PBMCs) in asthmatics using TRIzol reagents (Invitrogen) and then reverse transcribed into cDNA using M-MLV Reverse Transcription System (Promega). qRT-PCR was employed to analyze mRNA expression of IRAK-M by BIO-RAD CFX96 Real-Time PCR system using PowerUp SYBR Green Master Mix according to the manufacturer's instructions (ABI). Housekeeping gene glyceraldehyde-3-phosphate dehydrogenase (GAPDH) was used as internal controls to normalize IRAK-M mRNA expression. All reactions were carried out in triplicate. The qRT-PCR primers were: IRAK-M transcript variant 1 and 2 5' TCAGAGAAGAGTTATCAGGAAGGTG3', 3' AAGCTGATGGAAGATTTAAGCAGTA5'; IRAK-M transcript variant 2 5' TGGCTGGATGTTCGTCATATTG3', 3' CTCCTGGAGGACCTGTAAAAGGT5'; GAPDH 5' GGAGCGAGATCCCTCCAAAAT3', 3' GGCTGTTGTCATACTTCTCATGG5'.

Electrophoretic mobility shift assay (EMSA)

Allele-specific alteration in rs1624395 binding to transcription factor c-Jun was assayed by using EMSA. Nuclear protein c-Jun was prepared from Hela cells transfected with an expression pET-28α-His-MBP vector for c-Jun. EMSA were performed using double-stranded (ds) DNA probes. Sequences of oligonucleotides used were as follows. For IRAK-M rs1624395 allele A: Forward 5′- acagagcacagaggaggaaatgataacttggg-3′, Reverse, 5′-cccaagttatcatttcctcctctgtgctctgt −3′; For IRAK-M rs1624395 allele G: Forward 5′-acagagcacagaggagggaatgataacttggg −3′, Reverse 5′- cccaagttatcattccctcctctgtgctctgt-3′. The 5′-biotin-labeled probes were synthesized by Invitrogen.

To ensure specificity of DNA–protein binding, unlabeled probe was used in a 30-fold molar excess as a binding competitor before incubation of nuclear protein extracts with biotiny-labeled probes. LightShift chemiluminescent EMSA kit was used according to manufacturer's instructions (Thermo Fisher Scientific).

Animal

IRAK-M KO mice has been described elsewhere (16). IRAK-M KO mice (B6.129S1-Irak3^{tmlFlv}/J) were a kind gift by Dr. Nikolaos G. Frangogiannis (Albert Einstein College of Medicine) and Wild type (WT) mice (purchased from Experimental Animal Research Center, Beijing, China) with C57BL/6 background were maintained in a pathogen-free mouse facility at Peking Union Medical College Hospital Animal Care Center. 10–12 weeks old mice were used for experiments.

All experiments were performed according to international and institutional guidelines for animal care, and approved by Peking Union Medical College Hospital Ethics Committee for animal experimentation.

Chronic asthma mouse model

The chronic asthma model was established according to that previously reported with minor modifications (24, 27). Briefly, mice were given 50 μg of OVA (Grade V, Sigma, MO) absorbed to 2.25 mg aluminum hydroxide (alum) in 200 μl of sterile saline on days 0 and 13 by intraperitoneal (i.p.) injection, then challenged with 1% aerosolized OVA via a PARI nebulizer for 30 minutes daily from day 19 to day 24, then three times per week from day 26 to day 60. Sham mice received alum and were exposed to 0.9% NaCl solution alone. Mice were sacrificed 24 hours after the last challenge for further analysis.

Airway responsiveness

Airway responsiveness to inhaled Mch was determined in mice 24 hours after the final aerosol challenge as we have previously described (24, 28).

Lung histology

Mice were sacrificed and left lungs were taken out and inflated to 25 cmH_2O with 10% formalin, fixed overnight, then embedded in paraffin, and sectioned to 3 μm thickness. Hematoxylin & eosin (H&E), periodic acid-Schiff (PAS), and Masson Trichrome's (MT) stains were performed to evaluate the severity of airway inflammation, mucus secretion, and collagen deposit.

Histopathological scoring

Semiquantitative scoring for airway inflammation in H&E slides was evaluated in a blind manner by counting the inflammatory cell infiltrated around airways and vessels according to the previously reported (29). 0 = normal; 1 = <3 cell diameter thick; 2 = 4–10 cells thick; 3 = >10 cells thick. A score of 0–3 on each section was used to reflect overall extent of airway inflammation (0: normal; 1: <25% of each section; 2: 25– 75%; 3: >75%). The index was calculated by multiplying severity by overall extent with a maximal score of 9.

Mucus scoring was evaluated based on the previously published method (30). Mucous scores were: 0 - no mucous, 1 - a few cells secreting mucous, 2 - many cells secreting mucous, and 3 - extensive mucous production.

Bronchoalveolar lavage (BAL) fluid collection

Mouse trachea was cannulated with a 20-gauge catheter, through which 0.8 ml ice-cold PBS (pH 7.4) was used to lavage the lung for 3 times. The recovered fluid was centrifuged at 1500 rpm for 5 min at 4°C. Cytospins were prepared from cell pellets.

Cytokine analysis

Quantitative real-time RT-PCR (qRT-PCR) was used to reflect mRNA expression of cytokines, including IL-4, IL-13, IFNγ, cytotoxic lymphocyte antigen 4 (CLTA-4), and TGFβ1. Total RNA was prepared from the right lung of animal using TRIzol reagent, and reverse transcribed into complementary DNA (cDNA) using a commercial kit (TaKaRa). qRT-PCR was performed on the ABI 7500 Fast real time PCR System (Applied Biosystems) in a 20μl reaction that contained 2 μl of cDNA and SYBR Premix Ex Taq (TaKaRa). The

expression level of GAPDH was used as an internal control. The relative expression was calculated with the comparative Ct method using 7500 Software v2.0.6 (Applied Biosystems) and was expressed as the fold change compared to the control. The murine primers used to amplify genes were as follows: IRAK-M 5'GGGGCATCAACGAGCTATCC3', 3'GGTTCCAGAGGTCCAGGGTC5'; IL-4 5' TCGAATGTACCAGGAGCCATAT3', 3' GAAGCACCTTGGAAGCCCTA5'; IL-13 5' AGGCCAGCCCACAGTTCTA 3', 3' CCACCAAGGCAAGCAAGAG5'; IFNγ 5' GCTGATCCTTTGGACCCTCT3', 3' AGGCTTTCAATGACTGTGCC5', cytotoxic T-lymphocyte-associated protein 4 (CTLA-4) 5' TCCGGAGGTACAAAGCTCAACTG3', 3' ACCATGGCTGCTAGCCAACAC5'; TGF-β1 5' AATGGTGGACCGCAACAAC 3', 3' GCACTGCTTCCCGAATGTC5'; GAPDH 5' TTGTCTCCTGCGACTTCAACA3', 3' TGGTCCAGGGTTTCTTACTCC5'.

Commercial ELISA kits were employed to detect concentrations of IL-4, IL-13, and IFNγ in BAL fluid (R&D systems) and levels of IL-17A, IL-33, and Thymic stromal lymphopoietin (TSLP) in the supernatant of lung homogenates (eBioscience). Measurements of IL-10, IL-12p40, IL-23, and IL-27 were used by LEGENDplex (Biolegend).

Hydroxyproline assay

Total collagen contents in lung were determined by analysis of hydroxyproline. Hydroxyproline contents in lung were measured using a commercial kit (Jiancheng Bioengineering Company, Nanjing, China).

Western blotting

The whole protein from the lung was prepared as previously described with modifications (31). The lungs were harvested and homogenized in lysis buffer containing a protease inhibitor cocktail (Sigma). Cell debris was removed by centrifugation at 12 000×*g* for 10 min at 4°C. The supernatants were eluted by adding an equal volume of sample loading buffer, then run on 12% SDS-PAGE gels before transferring to PVDF membranes. Membranes were incubated in the presence of the indicated antibodies. Antibodies were as follows: anti-mouse IRAK-M (Abcam) and anti-mouse α-SMA (Boster, Wuhan, China). Primary antibody application was followed by incubation with horseradish peroxidase (HRP)-conjugated secondary antibodies (rabbit anti-mouse IgG) (Bioleaf, Shanghai, China). Immunopositive blots were visualized using an enhanced chemiluminescence with AlphaEase FC imaging system (Alpha Innotech, San Leandro, CA) and semi-quantitatively analyzed with AlphaEase® FC software (Alpha Innotech).

Flow cytometry analysis

Flow cytometry analysis was performed using single cell suspension. Single cell suspension was prepared according to the previously described (24). Briefly, instilled lungs and spleens were minced and digested with collagenase type 1A and type IV bovine pancreatic DNase, then passed through a cell strainer to obtain cell suspension. The mononuclear cells from lung and spleen were isolated by centrifugation with Ficoll solution.

Cells were incubated with fluorochrome (FITC, PE, PerCP-Cyanine5.5, APC)-conjugated Abs (Anti-Mouse CD4, CD8, ST2, MHC Class II,CD80, CD86, OX40L, Siglec-F, Ly-6G, CD3, OX40L, PD-L1, and PD-L2) at room temperature for 30 to 45 minutes. Cytokine intracellular staining was performed on cells that had been stimulated with 50 ng/ml of phorbol myristate acetate (Sigma-Aldrich) and 1 μM of ionomycin (Sigma-Aldrich) in the presence of GolgiStop (BD Biosciences) for 6 hours. The activated cells were fixed, permeabilized, and stained with mAbs (Anti-mouse IFN-γ, IL-4, IL-17A, T-bet, Foxp3 and ROR-γ). All samples were analyzed with BD Accuri C6 (BD). The fluorochrome-conjugated Abs were purchased from eBioscience/BD/Biolegend, and the corresponding isotype control Abs were added to “isotype samples” at the same concentrations as the Abs of interest.

Culture and purification of bone marrow-derived dendritic cells (BMDCs) and macrophages (BMDMs)

Bone marrow was obtained from C57BL/6 mice. The harvested bone marrow cells depleted of red blood cells were incubated for 7 days with RPMI 1640 containing 10% FBS, 100 U/ml penicillin, 100 U/ml streptomycin, 20 ng/ml GM-CSF (for BMDCs) or 50ng/ml GM-CSF (for BMDMs). Purification of BMDCs was used a CD11c magnetic cell-sorting kit (Miltenyi Biotec, Gladbach, Germany). BMDMs were recovered from the adherent cells by digestion with 5% trypsin. Stimulation of BMDCs/BMDMs was performed with lipopolysaccharide (LPS) (1μg/ml) on day 8 for 24h.

Statistical analysis

For association between IRAK-M SNPs and asthma susceptibility, all genotype and phenotype data were formatted using PLINK. Genotype and allele frequencies in cases and controls were compared by contingency table analysis. Genotype relative risk was calculated according to the statistical method described by Lathrop (17). Quantile normalization was applied to all quantitative traits. LD and haplotypes were assessed using the Haploview version 4.0 (32). All markers were included in these analyses on a gene-by-gene basis.

Comparisons of the animal data were performed using one-way ANOVA with Tukey post doc test for multiple groups and Student’s *t* test for two groups with GraphPad Prism Version 5.01 (GraphPad Software, La Jolla, California). Data are expressed as means ± SEM and a p-value < 0.05 was considered significant.

Results

IRAK-M SNPs and susceptibility to adult-onset asthma

Given the positive association of IRAK-M polymorphism with the susceptibility to early-onset asthma in children (11), we examined the impact of IRAK-M SNPs on the risk of developing adult-onset asthma. We selected nine IRAK-M SNPs that were studied in early-onset asthma (11). After correction for multiple tests, we found two IRAK-M SNPs, rs1624395 and rs1370128, were significantly associated with adult-onset asthma (OR=1.227, 95% CI=1.054 – 1.428, p=0.008 for rs1624395; OR=1.187, 95% CI=1.020 – 1.381, p=0.027 for rs1370128). Homozygote G/G for rs1624395 and homozygote C/C for

rs1370128 were more often seen in adult-onset asthma patients than in controls (p-values were 0.025 and 0.009, respectively) (Table 2). We also demonstrated the associations between polymorphic markers in IRAK-M locus and numerous quantitative asthma-related traits, for instance the marker rs7970350 with high blood eosinophils counts ($p < 0.05$), rs2141709 with airflow obstruction (FEV1% and FEV1/FVC%, all $p<0.05$), rs1821777 with FEV1% ($p<0.01$) and IgE level ($p<0.05$), and rs1624395 with IgE level ($p<0.05$).

Haplotypes analysis and linkage disequilibrium tests

Haplotype analyses of all markers on a gene-by-gene base (including haplotypes present in ≥ 5% of the genotyped population) revealed the significant association between one IRAK-M haplotype and asthma after 1000 permutations (GTAT, $\chi^2 = 0.787$, permutation p=0.0079). This haplotype was significantly under-represented in asthmatic cases in comparison with controls, with case and control frequencies being 0.098 and 0.138, respectively (Table 3). This haplotype therefore appears to confer protection against the risk of having asthma.

Influence of rs1624395 on mRNA expression of IRAK-M in circulating monocytes

The asthma susceptible genes contain polymorphisms that modify function. We next studied the functionality of the risk SNPs of IRAK-M influencing asthma susceptibility. We chose the top-associated polymorphism rs1624395, which is in linkage disequilibrium with rs1370128 ($r^2 = 0.9$) (Supplemental figure s1). We found that rs1624395 influenced the mRNA expression of IRAK-M transcript variant 1 in peripheral monocytes from asthma patients (n= 60, AA=30, AG+GG=30). As shown in Figure 1, asthmatics carrying AG/GG genotypes had significantly higher mRNA levels in blood monocytes than the AA genotype carriers.

Transcription factor binding property modulated by rs1624395

To define the possible molecular mechanism underlying the difference in mRNA expression of IRAK-M by PBMCs in asthmatics carrying rs1624395 A or G allele, we used EMSA analysis to detect the binding properties of rs1624395 G allele and A allele to nuclear factor C-Jun. C-Jun has been demonstrated to directly bind the human IRAK-M promoter to upregulate epithelial IRAK-M expression (22). Utilizing the 5’-biotinlynated probe against rs1624395 to co-incubate with nuclear factor c-Jun protein from human Hela cells, we demonstrated significantly greater affinity for allele G than allele A (Figures 2A and B).

IRAK-M expression in the mouse lungs following chronic OVA exposure

In an acute asthma mouse model, we have shown significantly higher mRNA expression of IRAK-M in the lungs exposed to OVA (around 50-fold) (24). We further examined the change of IRAK-M expression in a chronic asthma mouse model sensitized and challenged by OVA for two months (Figure 3A). The expression of IRAK-M mRNA was significantly higher (by ~ 100-fold) in mouse lungs with chronic OVA treatment than those with PBS treatment (Figure 3B, $p<0.01$). Consistently, a significantly higher level of lung IRAK-M protein was observed in chronically OVA-treated mice than PBS-treated mice (Figure 3C, $p<0.05$).

Effect of IRAK-M deficiency on chronic airway inflammation induced by OVA

In our previous study, we have demonstrated a clear inhibitory role of IRAK-M on the acute allergic airway inflammation with OVA asthmatic mouse model (24). However, this conclusion cannot be simply extrapolated to the regulation of chronic allergic inflammation, as the role of IRAK-M is known to vary between the acute and chronic inflammatory phases (25). Here, we further assessed the impact of IRAK-M on chronic asthma, with a simulated model established by repeated OVA administration (Figure 3A) to WT or IRAK-M KO mice. We first assessed the airway inflammation by examining the epithelial thickness and the inflammatory cell infiltration in the airway walls. We found no inflammation around the airways in PBS-treated WT or IRAK-M KO mice (Figure 4A, left panel). Following chronic OVA challenge, WT mice showed worse pathological characteristics of airway inflammation than IRAK-M KO mice did, such as thicker airway epithelia, heavier mucus production and more inflammatory cells around the bronchioles and vessels (Figure 4A, right panel). We semi-quantitatively scored the histopathological findings. The inflammation scores of WT mice were significantly higher than those of IRAK-M KO mice (3.28 ± 0.40 vs. 2.47 ± 0.39, $p < 0.05$) (Figure 4B). Consistently, the number of total inflammatory cells, eosinophils, neutrophils, lymphocytes, but not macrophages, in BAL fluid was significantly more in WT mice than IRAK-M KO mice (Figure 4C). Using flow cytometry analysis, we found a significantly higher percentage of Th2 cells in the BALF from WT mice than that in IRAK-M KO mice (Figure 4D), even though the percentages of total T cells or B cells were not different between the two groups.

Effect of IRAK-M ablation on airway remodeling after chronic OVA stimulation

Airway remodeling is one of characteristics of chronic asthma and related to airway obstruction (2, 33). We subsequently examined the impact of IRAK-M KO on airway reactivity and airway remodeling in mice of chronic OVA model. Following chronic OVA challenge, WT and IRAK-M KO mice developed increased airway resistance in response to the increasing concentrations of methacholine (MCh). Of note, the airway resistance was significantly higher in WT mice as compared to the IRAK-M KO mice ($p < 0.05$) (Figure 5A).

To reflect the effect of IRAK-M deficiency on airway pathology (33), we performed PAS scorings, MT staining, and a-SMA expression. We found that following chronic OVA challenge, 1) more severe mucus hypersecretion in the airways from the WT mice than that from IRAK-M KO mice (Figure 5B), 2) significant higher PAS scores in WT mice than IRAK-M KO mice (2.78 ± 0.44 vs. 1.84 ± 0.38, $p<0.05$) (Figure 5C), 3) more collagen deposition in the peribronchiolar area by MT staining and higher hydroxyproline content in the WT lungs than IRAK-M KO lungs (0.60 ± 0.11μg/mg vs. 0.41 ± 0.09 μg/mg, $p<0.05$) (Figure 5D), and 4) higher expression of α-SMA in WT lungs than IRAK-M KO lungs by Western blotting assay (Figure 5E).

Impact of IRAK-M deficiency on T cell subsets following chronic OVA stimulation

Asthma is typically characterized by Th2-type inflammation in the airways (7). However, the immune regulation of asthmatic inflammation involves a complex entity of T cell subtypes. Therefore, we further characterized the influence of IRAK-M KO on the

composition of T subsets in mouse lung homogenates and spleens of the chronic OVA model. As shown in Figure 6A, chronic OVA challenge resulted in an increased Th2 cell percentage and a reduced Th1 cell percentage in both WT and IRAK-KO mouse lungs. However, the changes in Th1 cell and Th2 cell percentage were significantly less in IRAK-M KO mouse lungs than WT mouse lungs. Additionally, we observed significantly higher percentage of Th1 cells in the spleens from OVA-treated IRAK-M KO mice than WT mice (Figure 6B). Moreover, chronic OVA treatment significantly increased the Th17 and Treg cell percentage in both IRAK-M KO and WT mouse lungs, with no significant inter-group difference (Figures 6A and 6B).

Effect of IRAK-M deficiency on cytokines production in response to chronic OVA stimulation

Asthmatic airway inflammation is mediated by cytokines produced from structural and immune cells (1). To understand the mechanisms by which IRAK-M support the Th2 immune responses following chronic OVA stimulation, we examined the levels of both proinflammatory and anti-inflammatory cytokines in BAL fluid and lungs of chronically immunized and challenged WT and IRAK-M KO mice.

The airway epithelium constitutes the first line of defense against the environmental stimuli. Upon exposure to an inhaled allergen, airway epithelial cells release the cytokines to induce resident DC maturation and further skew the naïve T cells differentiation to Th2 type (1, 34). In the acute mouse model of asthma, we have demonstrated OVA-induced elevation of epithelium-derived Th2 instructive cytokines, IL-17A, IL-33, and TSLP, with a higher level in the lungs of IRAK-M KO mice than WT mice (24). However, we didn't find a significant difference in the elevated concentrations of these cytokines in the lung homogenates between WT and IRAK-M KO mice following chronic OVA administration (Figure 7A).

At protein level, the concentrations of Th2 cytokine IL-4 and IL-10, not IL-13, were significantly higher in BAL fluid from chronically OVA-treated WT mice, whereas the concentration of Th1 cytokine IFNγ was significantly higher in BAL fluid from chronically OVA-treated IRAK-M KO mice (Figure 7B). Moreover, we found that chronic OVA-stimulation caused significantly higher levels of IL-12p40, IL-23, and IL-27 in BAL fluid from IRAK-M KO mice than those from WT mice. At mRNA level, lung expression of IL-4 and IL-13 was significantly increased in WT mouse lungs, but not in IRAK-M KO mouse lungs, by chronic OVA stimulation. By contrast, mRNA expression of IFNγ and CLTA-4 in the lungs was significantly elevated in IRAK-M KO mice (Figure 7C). Transforming growth factor β 1 (TGF-β1), increased in the airways of patients with asthma (35, 36), mediates the association between airway remodeling and AHR during asthmatic process (37), In supporting of this finding, we found that lung expression of TGF-β1 mRNA was significantly enhanced by chronic OVA challenge in WT mice, but not in IRAK-M KO mice (Figure 7C). Together, these data suggested IRAK-M KO suppressed the Th2 inflammation and promoted Th1 phenotype exampled by a greater INF-γ production.

Effect of IRAK-M deficiency on expression of costimulatory molecules on DCs and macrophages

To further understand the mechanism underlying the suppression of chronic allergic airway inflammation by IRAK-M knockout, we further evaluated the function of IRAK-M KO antigen-present cells (APC) in the chronic asthmatic inflammation.

Airway APC cells, mainly DCs and macrophages, play crucial roles not only to initiate the specific Th2 cell immune responses but also to re-stimulate local residential T (memory) lymphocytes and recruit effector cells following the repeated allergen exposure (1, 34). We have previously demonstrated that IRAK-M KO led to a downregulation of costimulatory molecules, such as OX40L, CD80, CD86, and CD124, on the airway APCs in acute asthma model of mice (24). However, in the present study of chronic OVA model of asthma, we found that IRAK-M KO did not make a difference on the expression of costimulatory molecules MHC II, CD80, and CD86 on lung DCs in spite of a higher expression of CD80 by airway macrophages of IRAK-M KO mice (Supplemental figure s2). Notably, the expression of PD-L1 (CD274) and PD-L2 (CD273) was significantly higher on the lung DCs from IRAK-M KO mice than WT mice after chronic OVA exposure ((Figure 8A, $p<0.05$). Similarly, a higher surface expression of PD-L1 (CD274) was revealed on the BALF macrophages from IRAK-M KO mice as compared to WT mice (Figure 8B).

In vitro effect of IRAK-M KO on activity of bone marrow-derived dendritic cells (BMDC) and bone marrow-derived macrophage (BMDM)

To confirm that the absence of IRAK-M modifies the instructive role of APCs on T cell responses, we examined the cytokines released by activated WT and IRAK-M KO dendritic cells and macrophages. We utilized BMDCs and BMDMs, stimulated them with LPS, a specific TLR4 agonist. We found that LPS induced a significant elevation of IRAK-M expression on WT BMDCs and BMDM (Figure 9A).

A lack of IRAK-M did not make a difference in the CD124, CD206, and OX40L expression of BMDC or BMDM to LPS stimulation (data not shown). Instead, IRAK-M KO led to a significantly higher level of IFNγ, TNFα, and IL-6 production by BMDCs and BMDMs to LPS stimulation (Figures 9B and 9C). We did not find a significant difference in the LPS induced IL-13 production between WT and IRAK-M KO BMDCs or BMDMs (data not shown). These data support that loss function of IRAK-M in DCs or macrophages favors Th1 promotion.

Discussion

In this present study, we reported an association of two IRAK-M SNPs, rs1642395 and rs1370128, with susceptibility to adult-onset asthma and one haplotype (GTAT) of IRAK-M potentially protecting against the risk of asthma. These findings provide evidence for the hypothesis that IRAK-M plays a role in the pathogenesis of adult-onset asthma. It is by far the first genetic study of IRAK-M as an adult-onset asthma susceptible gene in Han Chinese ethnicity and provides invaluable supplementary information to the comprehensive role of IRAK-M in the pathogenesis of asthma.

The susceptible IRAK-M SNPs reported in this study are different to the original findings from early-onset persistent asthmatic patients (11). Several factors could attribute to the discrepancy. Firstly, the patient age, ethnicity, and disease stage are different among the study groups. Asthma susceptibility is the result of interaction of genetic profiles and environmental factors at various times throughout the entire life. Some susceptible genes were reported to cause early onset mild or intermittent asthma under the risk environmental exposure (6). Genetic evidence has shown different gene expression profiles in the airways between adult- and childhood-onset severe asthma (38). Moreover, case-control association and next-generation sequencing studies have revealed significant discrepancies in the frequencies of SNPs and haplotype blocks for asthma genes between Chinese and other ethnicities (39). Secondly, the inconsistencies among studies could reflect real differences of genetic effects of IRAK-M variants or linkage disequilibrium patterns between typed and true causative variants (11, 14, 40). Also, we found in the present study that genetic markers in IRAK-M were closely associated with asthma susceptibility, but not linked to asthma-related phenotypes. A similar phenomenon has been reported in the previous genetic studies of the asthmatic populations (6).

Many asthma-associated SNPs are located in non-coding intergenic and intronic regulatory regions. These SNPs may modify mRNA expression, transcription factor binding (41, 42). In the present study, we analyzed the top-associated SNP rs164395 and identified the risk allele G that linked to significantly higher mRNA expression of IRAK-M in PBMCs from asthmatics. Using EMSA, we reveal the potential underlying mechanism is that G allele, as compared to A allele, has a higher binding capacity to C-Jun, a transcription factor directly binding to the human IRAK-M promoter (22).

IRAK-M is known to regulate the cytokine production of monocytes/ macrophages via intervening the intracellular the TLR/NF-κB signaling pathway (16). We have previously reported that IRAK-M deficiency exacerbated the OVA-induced acute airway inflammation through multiple pathways, such as promoting the production of proinflammatory cytokines by airway epithelial cells, enhancing the activities of DCs and macrophages, and deviating the CD4+ T cells differentiation to Th2 and Th17 cells (24). But, in the present study, we demonstrated an inhibitory effect of IRAK-M deficiency on the OVA-induced chronic mouse airway inflammation. Mechanistically, we found that IRAK-M KO could reduce the Th2/Th1 imbalance in the chronic allergic inflammation by increasing the Th1 cell percentage and Th1 cytokines (IFNγ, IL-12p40, IL-23, IL-27) production. The enhanced Th1 function can inhibit the Th2 cell proliferation and activity (1). Indeed, constant overexpression of airway epithelial IRAK-M could impair the innate immunity and compromise the capability of clearance of inhaled environmental antigens from the airways (22, 23, 43). Chronic stimulation of innate immunity is a major contributor to the persistent airway inflammation, and irreversible airway remodeling (1, 34). At cellular level, our *in vitro* data demonstrated IRAK-M KO BMDCs and BMDMs secreted more Th1 cytokines after TLR ligation by LPS. A similar finding that IRAK-M inhibited the Th1 cytokine production by DCs has been reported previously (44). Hence, the impact of IRAK-M KO on the chronic allergic airway inflammation could attribute to the alternation of DC/ macrophage- medicated T cell differentiation.

The mechanism underlying the distinct regulation of IRAK-M on the DC function at different inflammatory stages is not clear. Our studies suggested it could act via modulating the co-stimulatory signaling molecules on the DCs differentially. There is mounting evidence demonstrating that differentiation of T helper cells relies on particular costimulatory molecules signaling from APCs (45). In the present study, we observed that IRAK-M KO led to a significantly higher expression of PD-L1 (CD274) and PD-L2 (CD273) on the lung DCs or macrophages following chronic OVA stimulation. The surface molecules PD-L1 (CD274) and PD-L2 (CD273) of DCs were known to present the inhibitory signal to T cell activation (46). Particularly, PD-L2 (CD273) was shown to attenuate Th2-predominat allergic response through an IFNγ-dependent mechanism (47). Previous studies have demonstrated that CTLA-4, interacting with CD80, inhibited Th2 differentiation (48, 49). In supporting with these findings, our data showed that IRAK-M KO mice had a higher expression of CTLA-4 mRNA by lung and CD80 by airway macrophages after chronic OVA challenge.

In addition, IRAK-M also regulates the tissue remodeling process accompanying chronic inflammation. In an animal model of bleomycin-induced lung injury, IRAK-M was shown to promote inflammatory responses and collagen deposit in the lungs at the late stage (20). In another study of cardiac remodeling following myocardial infarction, IRAK-M was demonstrated to prompt the myofibroblast conversion via inducing the TGF-β1 mediated α-SMA expression in the fibroblasts (50). Similarly, in the present study, we found that IRAK-M loss attenuated the airway remodeling and reduced the α-SMA and TGFβ1 expression in the lung tissue with chronic allergic airway inflammation.

Our study has a few limitations. For instance, this study only included adult patients and lacked children asthmatics as replicating control. Therefore, we cannot conclude if the polymorphisms of IRAK-M identified in this study are an age-specific risk of asthma susceptibility or asthma-related traits. However, this current study demonstrated the functionalities of these two associated IRAK-M SNPs, suggesting the importance of IRAK-M in asthma pathogenesis. Besides, the mice used in this study underwent whole-body IRAK-M KO which might introduce some unrecognized confounding variables to impact the experimental results, an allelic-specific and temporally controllable knockout model, as well as an overexpression animal model is desired to precisely study the complexity of asthma.

In conclusion, we demonstrated in the present study that IRAK-M was genetically linked in adult-onset human asthmatics and it has a pro-inflammatory effect in an animal model using mouse lungs following chronic allergen stimulation. This action of IRAK-M is opposite to its anti-inflammatory effect in the acute phase of asthma. The underlying mechanism of these findings is related to promoting effect of IRAK-M on DC-mediated, Th2-deviated immune activation following a repetitive allergen stimulation. These findings illustrated the complexity of immune regulation at different stages of asthmatic inflammation. Moreover, it implicates that down-regulating IRAK-M and the downstream signaling pathway may provide an alternative therapy to control chronic asthmatic airway inflammation.

Supplementary Material

Refer to Web version on PubMed Central for supplementary material.

Acknowledgments

The authors would like to thank Professor Nikolaos G. Frangogiannis for kindly gifting IRAK-M knockout mice. The authors would like to thank all subjects for agreeing to participate in this study. We thank Dr. Kewu Huang for the help in the FlexiVent measurement of airway reactivity. The authors thank Prof. Roy Pleasants for his English editing.

Funding: This work was supported by grants from National Natural Sciences Foundation of China (Nos. 81170040, 81470229, and 30470767) and National Institutes of Health (K08HL135443). The sponsors had no role in study design, data collection and interpretation, and manuscript draft.

Abbreviations used

IRAK	IL-1 receptor associated kinase
TLR	toll-like receptor
AHR	airway hyperresponsiveness
KO	knockout
WT	wild type
Mch	Methacholine
BAL	bronchoalveolar lavage
GAPDH	glyceraldehydes-3-phosphate dehydrogenase
qRT-PCR	quantitative real-time PCR
BMDC	bone marrow-derived dendritic cell
BMDM	bone marrow-derived macrophage
OVA	ovalbumin
APC	antigen-presenting cell
PD-L1	programmed death-ligand 1
PD-L2	programmed death-ligand-2
TSLP	thymic stromal lymphopoietin
FEV1	forced expiratory volume in first second
FVC	forced vital capacity
SNP	single nucleotide polymorphism

References

1. Lambrecht BN, and Hammad H. The immunology of asthma. Nat Immunol 16: 45–56. [PubMed: 25521684]
2. Ojiaku CA, Cao G, Zhu W, Yoo EJ, Shumyatcher M, Himes BE, An SS, and Panettieri RA, Jr. TGF-beta1 Evokes Human Airway Smooth Muscle Cell Shortening and Hyperresponsiveness via Smad3. Am J Respir Cell Mol Biol.
3. Siroux V, Basagana X, Boudier A, Pin I, Garcia-Aymerich J, Vesin A, Slama R, Jarvis D, Anto JM, Kauffmann F, and Sunyer J. Identifying adult asthma phenotypes using a clustering approach. Eur Respir J 38: 310–317. [PubMed: 21233270]
4. Siroux V, Gonzalez JR, Bouzigon E, Curjuric I, Boudier A, Imboden M, Anto JM, Gut I, Jarvis D, Lathrop M, Omenaas ER, Pin I, Wjst M, Demenais F, Probst-Hensch N, Kogevinas M, and Kauffmann F. Genetic heterogeneity of asthma phenotypes identified by a clustering approach. Eur Respir J 43: 439–452. [PubMed: 24311777]
5. Zhang Y, Moffatt MF, and Cookson WO. Genetic and genomic approaches to asthma: new insights for the origins. Curr Opin Pulm Med 18: 6–13. [PubMed: 22112999]
6. Meyers DA, Bleecker ER, Holloway JW, and Holgate ST. Asthma genetics and personalised medicine. Lancet Respir Med 2: 405–415. [PubMed: 24794577]
7. Wenzel SE Emergence of Biomolecular Pathways to Define Novel Asthma Phenotypes. Type-2 Immunity and Beyond. Am J Respir Cell Mol Biol 55: 1–4. [PubMed: 27164162]
8. Stein MM, Hrusch CL, Gozdz J, Igartua C, Pivniouk V, Murray SE, Ledford JG, Marques Dos Santos M, Anderson RL, Metwali N, Neilson JW, Maier RM, Gilbert JA, Holbreich M, Thorne PS, Martinez FD, von Mutius E, Vercelli D, Ober C, and Sperling AI. Innate Immunity and Asthma Risk in Amish and Hutterite Farm Children. N Engl J Med 375: 411–421. [PubMed: 27518660]
9. Yokouchi Y, Nukaga Y, Shibasaki M, Noguchi E, Kimura K, Ito S, Nishihara M, Yamakawa-Kobayashi K, Takeda K, Imoto N, Ichikawa K, Matsui A, Hamaguchi H, and Arinami T. 2000 Significant evidence for linkage of mite-sensitive childhood asthma to chromosome 5q31-q33 near the interleukin 12 B locus by a genome-wide search in Japanese families. Genomics 66: 152–160. [PubMed: 10860660]
10. Raby BA, Silverman EK, Lazarus R, Lange C, Kwiatkowski DJ, and Weiss ST. 2003 Chromosome 12q harbors multiple genetic loci related to asthma and asthma-related phenotypes. Hum Mol Genet 12: 1973–1979. [PubMed: 12913068]
11. Balaci L, Spada MC, Olla N, Sole G, Loddo L, Anedda F, Naitza S, Zuncheddu MA, Maschio A, Altea D, Uda M, Pilia S, Sanna S, Masala M, Crisponi L, Fattori M, Devoto M, Doratiotto S, Rassu S, Mereu S, Giua E, Cadeddu NG, Atzeni R, Pelosi U, Corrias A, Perra R, Torrazza PL, Pirina P, Ginesu F, Marcias S, Schintu MG, Del Giacco GS, Manconi PE, Malerba G, Bisognin A, Trabetti E, Boner A, Pescollderungg L, Pignatti PF, Schlessinger D, Cao A, and Pilia G. 2007 IRAK-M is involved in the pathogenesis of early-onset persistent asthma. Am J Hum Genet 80: 1103–1114. [PubMed: 17503328]
12. Nakashima K, Hirota T, Obara K, Shimizu M, Jodo A, Kameda M, Doi S, Fujita K, Shirakawa T, Enomoto T, Kishi F, Yoshihara S, Matsumoto K, Saito H, Suzuki Y, Nakamura Y, and Tamari M. 2006 An association study of asthma and related phenotypes with polymorphisms in negative regulator molecules of the TLR signaling pathway. J Hum Genet 51: 284–291. [PubMed: 16432636]
13. Beygo J, Parwez Q, Petrasch-Parwez E, Epplen JT, and Hoffjan S. 2009 No evidence of an association between polymorphisms in the IRAK-M gene and atopic dermatitis in a German cohort. Mol Cell Probes 23: 16–19. [PubMed: 19013233]
14. Pino-Yanes M, Sanchez-Machin I, Cumplido J, Figueroa J, Torres-Galvan MJ, Gonzalez R, Corrales A, Acosta-Fernandez O, Garcia-Robaina JC, Carrillo T, Sanchez-Palacios A, Villar J, Hernandez M, and Flores C. IL-1 receptor-associated kinase 3 gene (IRAK3) variants associate with asthma in a replication study in the Spanish population. J Allergy Clin Immunol 129: 573–575, 575 e571–510. [PubMed: 22070913]
15. Pino-Yanes M, Ma SF, Sun X, Tejera P, Corrales A, Blanco J, Perez-Mendez L, Espinosa E, Muriel A, Blanch L, Garcia JG, Villar J, and Flores C. Interleukin-1 receptor-associated kinase 3 gene

associates with susceptibility to acute lung injury. Am J Respir Cell Mol Biol 45: 740–745. [PubMed: 21297081]

16. Kobayashi K, Hernandez LD, Galan JE, Janeway CA, Jr., Medzhitov R, and Flavell RA. 2002 IRAK-M is a negative regulator of Toll-like receptor signaling. Cell 110: 191–202. [PubMed: 12150927]
17. Baines KJ, Fu JJ, McDonald VM, and Gibson PG. Airway gene expression of IL-1 pathway mediators predicts exacerbation risk in obstructive airway disease. Int J Chron Obstruct Pulmon Dis 12: 541–550. [PubMed: 28223794]
18. Jenkins BJ Multifaceted Role of IRAK-M in the Promotion of Colon Carcinogenesis via Barrier Dysfunction and STAT3 Oncoprotein Stabilization in Tumors. Cancer Cell 29: 615–617. [PubMed: 27165738]
19. Gong H, Liu T, Chen W, Zhou W, and Gao J. Effect of IRAK-M on Airway Inflammation Induced by Cigarette Smoking. Mediators Inflamm 2017: 6506953. [PubMed: 28951634]
20. Ballinger MN, Newstead MW, Zeng X, Bhan U, Mo XM, Kunkel SL, Moore BB, Flavell R, Christman JW, and Standiford TJ. IRAK-M promotes alternative macrophage activation and fibroproliferation in bleomycin-induced lung injury. J Immunol 194: 1894–1904.
21. Steiger S, Kumar SV, Honarpisheh M, Lorenz G, Gunthner R, Romoli S, Grobmayr R, Susanti HE, Potempa J, Koziel J, and Lech M. Immunomodulatory Molecule IRAK-M Balances Macrophage Polarization and Determines Macrophage Responses during Renal Fibrosis. J Immunol 199: 1440–1452.
22. Wu Q, Jiang D, Smith S, Thaikoottathil J, Martin RJ, Bowler RP, and Chu HW. IL-13 dampens human airway epithelial innate immunity through induction of IL-1 receptor-associated kinase M. J Allergy Clin Immunol 129: 825–833 e822. [PubMed: 22154382]
23. Wu Q, van Dyk LF, Jiang D, Dakhama A, Li L, White SR, Gross A, and Chu HW. Interleukin-1 receptor-associated kinase M (IRAK-M) promotes human rhinovirus infection in lung epithelial cells via the autophagic pathway. Virology 446: 199–206. [PubMed: 24074582]
24. Zhang M, Chen W, Zhou W, Bai Y, and Gao J. Critical Role of IRAK-M in Regulating Antigen-Induced Airway Inflammation. Am J Respir Cell Mol Biol 57: 547–559. [PubMed: 28665693]
25. Hubbard LL, and Moore BB. IRAK-M regulation and function in host defense and immune homeostasis. Infect Dis Rep 2.
26. Amelink M, de Groot JC, de Nijs SB, Lutter R, Zwinderman AH, Sterk PJ, ten Brinke A, and Bel EH. Severe adult-onset asthma: A distinct phenotype. J Allergy Clin Immunol 132: 336–341. [PubMed: 23806634]
27. Lee SH, Eren M, Vaughan DE, Schleimer RP, and Cho SH. A plasminogen activator inhibitor-1 inhibitor reduces airway remodeling in a murine model of chronic asthma. Am J Respir Cell Mol Biol 46: 842–846. [PubMed: 22323366]
28. Lin Y, Yan H, Xiao Y, Piao H, Xiang R, Jiang L, Chen H, Huang K, Guo Z, Zhou W, Lu B, and Gao J. Attenuation of antigen-induced airway hyperresponsiveness and inflammation in CXCR3 knockout mice. Respir Res 12: 123. [PubMed: 21939519]
29. Willis CR, Siegel L, Leith A, Mohn D, Escobar S, Wannberg S, Misura K, Rickel E, Rottman JB, Comeau MR, Sullivan JK, Metz DP, Tocker J, and Budelsky AL. IL-17RA Signaling in Airway Inflammation and Bronchial Hyperreactivity in Allergic Asthma. Am J Respir Cell Mol Biol 53: 810–821. [PubMed: 25919006]
30. Wittke A, Weaver V, Mahon BD, August A, and Cantorna MT. 2004 Vitamin D receptor-deficient mice fail to develop experimental allergic asthma. J Immunol 173: 3432–3436. [PubMed: 15322208]
31. Liu ZJ, Yang YJ, Jiang L, Xu YC, Wang AX, Du GH, and Gao JM. Tyrosine sulfation in N-terminal domain of human C5a receptor is necessary for binding of chemotaxis inhibitory protein of Staphylococcus aureus. Acta Pharmacol Sin 32: 1038–1044.
32. Barrett JC, Fry B, Maller J, and Daly MJ. 2005 Haploview: analysis and visualization of LD and haplotype maps. Bioinformatics 21: 263–265. [PubMed: 15297300]
33. Davies DE, Wicks J, Powell RM, Puddicombe SM, and Holgate ST. 2003 Airway remodeling in asthma: new insights. J Allergy Clin Immunol 111: 215–225; quiz 226. [PubMed: 12589337]

34. Lambrecht BN, and Hammad H. Dendritic cell and epithelial cell interactions at the origin of murine asthma. Ann Am Thorac Soc 11 Suppl 5: S236–243. [PubMed: 25525726]
35. Redington AE, Madden J, Frew AJ, Djukanovic R, Roche WR, Holgate ST, and Howarth PH. 1997 Transforming growth factor-beta 1 in asthma. Measurement in bronchoalveolar lavage fluid. Am J Respir Crit Care Med 156: 642–647. [PubMed: 9279252]
36. Vignola AM, Chanez P, Chiappara G, Merendino A, Pace E, Rizzo A, la Rocca AM, Bellia V, Bonsignore G, and Bousquet J. 1997 Transforming growth factor-beta expression in mucosal biopsies in asthma and chronic bronchitis. Am J Respir Crit Care Med 156: 591–599. [PubMed: 9279245]
37. Ojiaku CA, Yoo EJ, and Panettieri RA, Jr. Transforming Growth Factor beta1 Function in Airway Remodeling and Hyperresponsiveness. The Missing Link? Am J Respir Cell Mol Biol 56: 432–442. [PubMed: 27854509]
38. Hekking PP, Loza MJ, Pavlidis S, de Meulder B, Lefaudeux D, Baribaud F, Auffray C, Wagener AH, Brinkman PI, Lutter RI, Bansal AT, Sousa AR, Bates SA, Pandis Y, Fleming LJ, Shaw DE, Fowler SJ, Guo Y, Meiser A, Sun K, Corfield J, Howarth PH, Bel EH, Adcock IM, Chung KF, Djukanovic R, and Sterk PJ. Pathway discovery using transcriptomic profiles in adult-onset severe asthma. J Allergy Clin Immunol.
39. Leung TF, Ko FW, Sy HY, Tsui SK, and Wong GW. Differences in asthma genetics between Chinese and other populations. J Allergy Clin Immunol 133: 42–48. [PubMed: 24188974]
40. Gabriel SB, Schaffner SF, Nguyen H, Moore JM, Roy J, Blumenstiel B, Higgins J, DeFelice M, Lochner A, Faggart M, Liu-Cordero SN, Rotimi C, Adeyemo A, Cooper R, Ward R, Lander ES, Daly MJ, and Altshuler D. 2002 The structure of haplotype blocks in the human genome. Science 296: 2225–2229. [PubMed: 12029063]
41. Hindorff LA, Sethupathy P, Junkins HA, Ramos EM, Mehta JP, Collins FS, and Manolio TA. 2009 Potential etiologic and functional implications of genome-wide association loci for human diseases and traits. Proc Natl Acad Sci U S A 106: 9362–9367. [PubMed: 19474294]
42. Maurano MT, Humbert R, Rynes E, Thurman RE, Haugen E, Wang H, Reynolds AP, Sandstrom R, Qu H, Brody J, Shafer A, Neri F, Lee K, Kutyavin T, Stehling-Sun S, Johnson AK, Canfield TK, Giste E, Diegel M, Bates D, Hansen RS, Neph S, Sabo PJ, Heimfeld S, Raubitschek A, Ziegler S, Cotsapas C, Sotoodehnia N, Glass I, Sunyaev SR, Kaul R, and Stamatoyannopoulos JA. Systematic localization of common disease-associated variation in regulatory DNA. Science 337: 1190–1195.
43. Wu Q, Martin RJ, Lafasto S, Efaw BJ, Rino JG, Harbeck RJ, and Chu HW. 2008 Toll-like receptor 2 down-regulation in established mouse allergic lungs contributes to decreased mycoplasma clearance. Am J Respir Crit Care Med 177: 720–729. [PubMed: 18202345]
44. Turnis ME, Song XT, Bear A, Foster AE, Gottschalk S, Brenner MK, Chen SY, and Rooney CM. 2010 IRAK-M removal counteracts dendritic cell vaccine deficits in migration and longevity. J Immunol 185: 4223–4232. [PubMed: 20817880]
45. Singh AK, Stock P, and Akbari O. 2011 Role of PD-L1 and PD-L2 in allergic diseases and asthma. Allergy 66: 155–162. [PubMed: 20722638]
46. Freeman GJ, Long AJ, Iwai Y, Bourque K, Chernova T, Nishimura H, Fitz LJ, Malenkovich N, Okazaki T, Byrne MC, Horton HF, Fouser L, Carter L, Ling V, Bowman MR, Carreno BM, Collins M, Wood CR, and Honjo T. 2000 Engagement of the PD-1 immunoinhibitory receptor by a novel B7 family member leads to negative regulation of lymphocyte activation. J Exp Med 192: 1027–1034. [PubMed: 11015443]
47. Matsumoto K, Inoue H, Nakano T, Tsuda M, Yoshiura Y, Fukuyama S, Tsushima F, Hoshino T, Aizawa H, Akiba H, Pardoll D, Hara N, Yagita H, Azuma M, and Nakanishi Y. 2004 B7-DC regulates asthmatic response by an IFN-gamma-dependent mechanism. J Immunol 172: 2530–2541. [PubMed: 14764726]
48. Oosterwegel MA, Mandelbrot DA, Boyd SD, Lorsbach RB, Jarrett DY, Abbas AK, and Sharpe AH. 1999 The role of CTLA-4 in regulating Th2 differentiation. J Immunol 163: 2634–2639. [PubMed: 10453003]
49. Bour-Jordan H, Grogan JL, Tang Q, Auger JA, Locksley RM, and Bluestone JA. 2003 CTLA-4 regulates the requirement for cytokine-induced signals in T(H)2 lineage commitment. Nat Immunol 4: 182–188. [PubMed: 12524538]

50. Saxena A, Shinde AV, Haque Z, Wu YJ, Chen W, Su Y, and Frangogiannis NG. The role of Interleukin Receptor Associated Kinase (IRAK)-M in regulation of myofibroblast phenotype in vitro, and in an experimental model of non-reperfused myocardial infarction. J Mol Cell Cardiol 89: 223–231. [PubMed: 26542797]

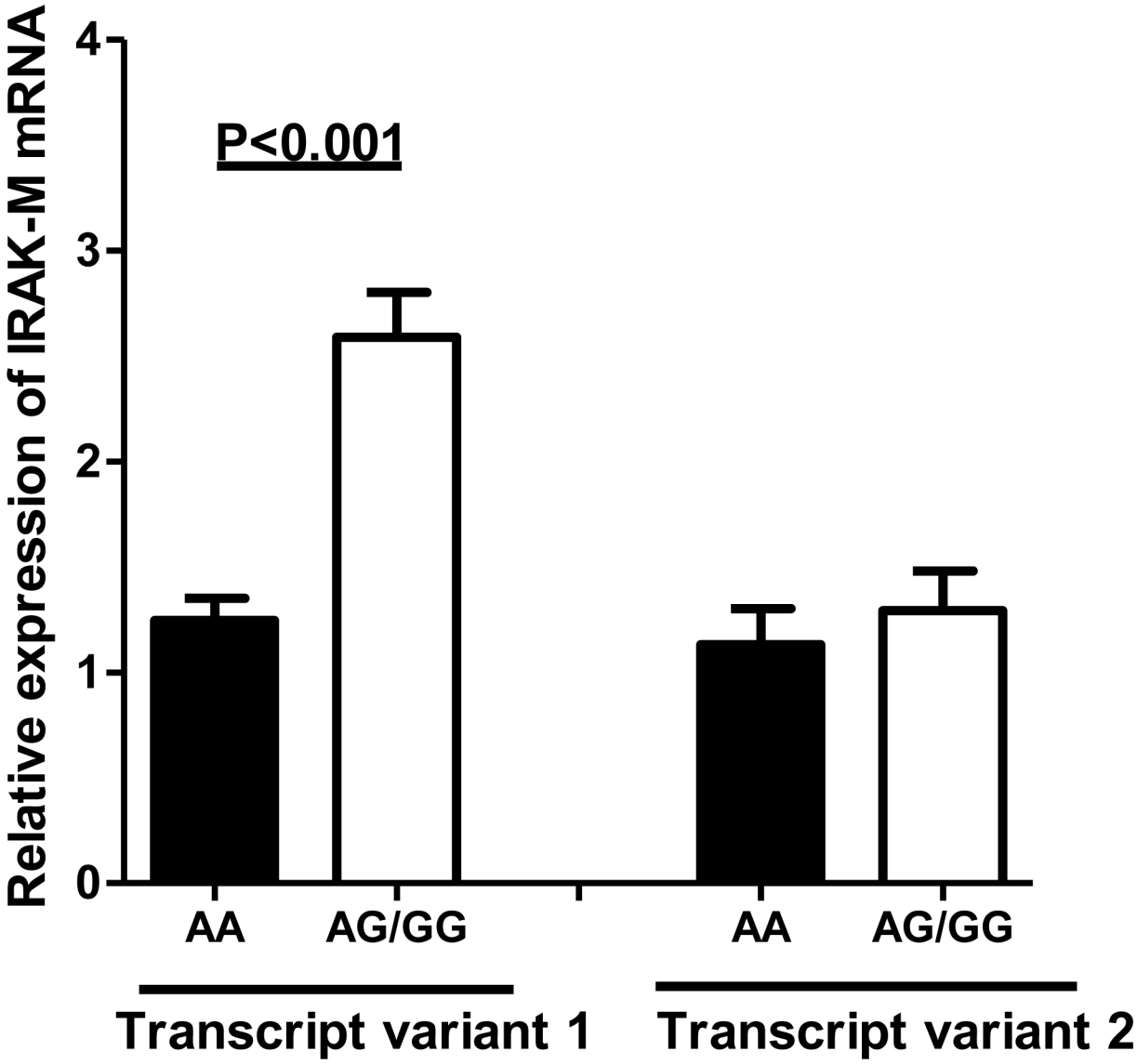

Figure 1. mRNA expression of IRAK-M carrying rs1624395 in circulating monocytes of asthmatics.

The allele-specific RNA expression of 2 transcriptional variants of IRAK-M carrying rs1624395 was quantified in PBMCs from asthma patients. Each sample was analyzed in triplicate. The results were normalized to the expression level of GADPH. N for AA group =30, AG/GG = 30. Data were expressed as mean ± SEM.

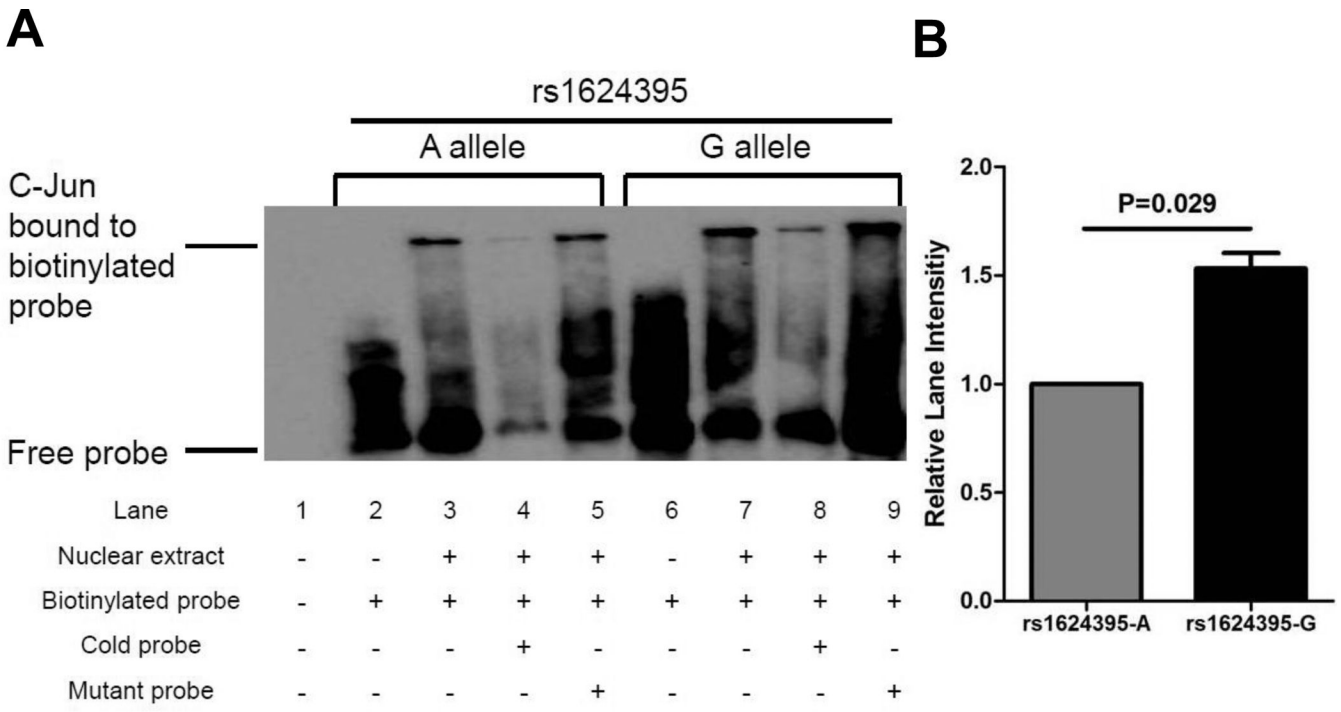

Figure 2. Enhanced binding of rs1642395 allele G to the nuclear protein C-Jun.

A. A representative image showing the A or G allele of rs1642395 bound to the C-Jun from Hela cells in the absence of competitor (Lane 3 and 7) or in the presence of cold probe (Lane 4 and 8) or mutant probe (Lane 5 and 9) by EMSA analysis. B. The summary plot of lane intensity to reflect the quantity of binding complex of c-Jun and allele A or G. The result was normalized to the intensity of the total signal in the corresponding lanes. Data were expressed as mean ± SEM, quantified for 3 replicates from Hela cells in each column.

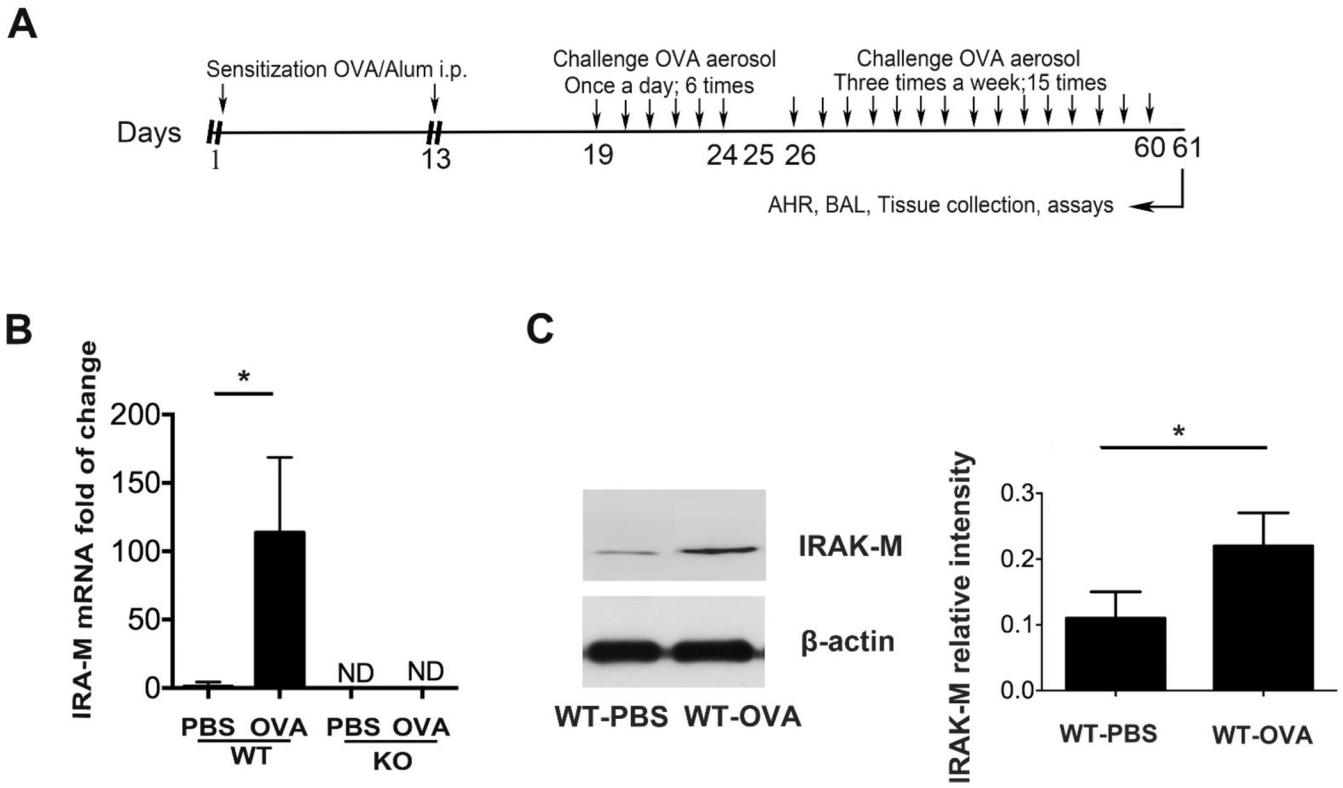

Figure 3. Increased expression of IRAK-M in lungs of mice after chronic OVA induction.

A. Schematic representation of the protocol to establish the chronic asthma mouse model with OVA stimulation. B. mRNA expression of IRAK-M in the lung of wild-type (WT) mice following chronic PBS or OVA treatment. IRAK-M gene expression was normalized to GAPDH expression, n=6–8 mice in each group. *, $p<0.01$. C. A representative Western-blot image (left panel) and summary plot (right panel) of IRAK-M protein expression in the lung of WT mice following chronic OVA or PBS stimulation. IRAK-M protein expression normalized to β-actin expression. n=6 mice in each group. *, $p<0.05$.

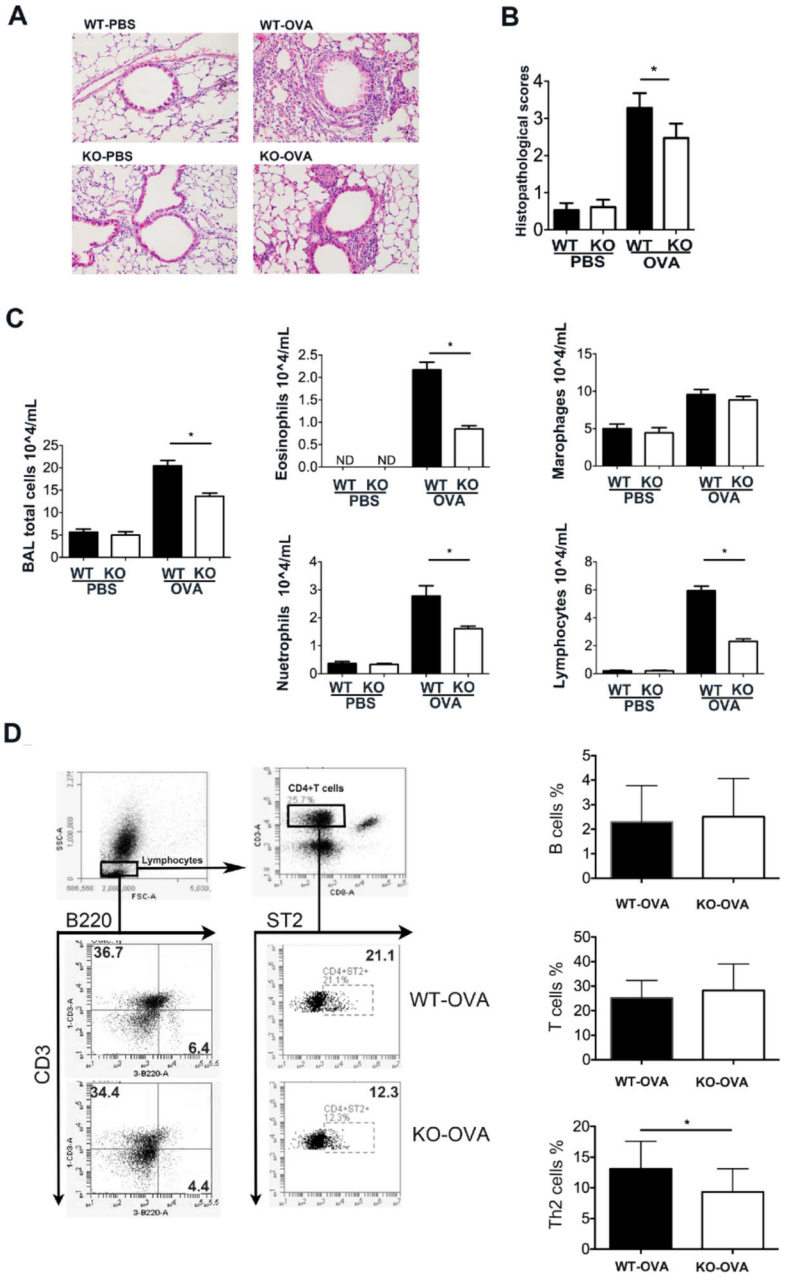

Figure 4. Attenuated airway inflammation in IRAK-M KO mice after chronic induction of OVA.

(A) Representative photomicrographs of hematoxylin- & eosin-stained lung tissues showing that OVA-sensitized and -challenged WT mice exhibited the typical pathological characteristics of chronic airway inflammation evidenced by thickened airway epithelium and more inflammatory cells in the peribronchial area and around vessels, compared with the similarly-treated IRAK-M KO mice. Original magnification ×20. (B) Semiquantitative histopathological scores from PBS- or OVA-treated WT and IRAK-M KO mice. n = 6 mice in each group; *p < 0.05. (C) Total inflammatory cells and differential subpopulations in BAL fluids, *, $p < 0.05$. (D) A representative image (left panel) and summary plots (right panel) showing the flow cytometry analysis of T, B cells and Th2 cell percentage in the

BALF from WT or IRAK-M KO mice following chronic OVA stimulation. n = 7–10 mice in each group; *$p < 0.05$.

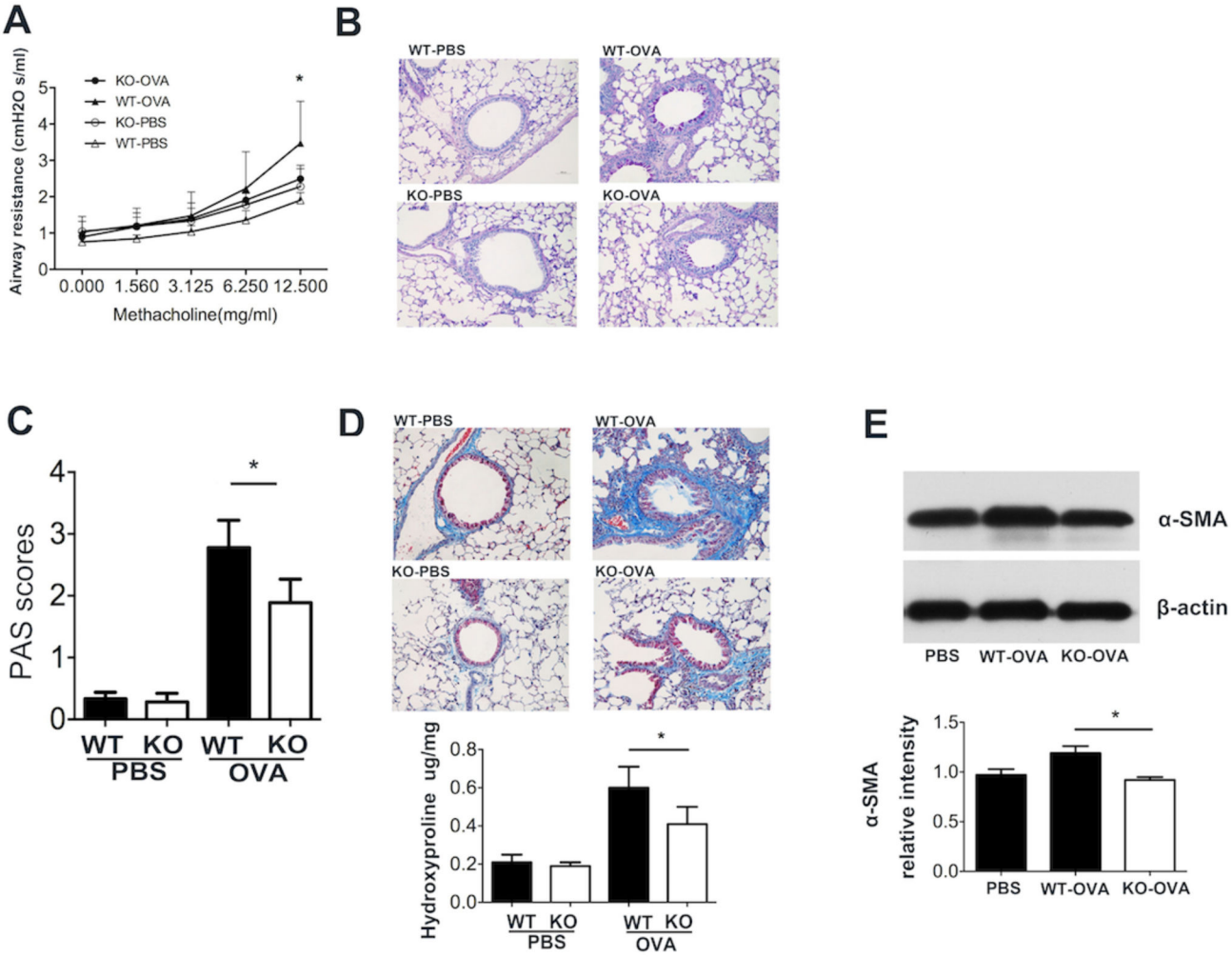

Figure 5. Reduction in airway hyperresponsiveness, mucus production, and airway remodeling in IRAK-M KO mice after chronic induction of OVA.

(A) Sensitized and challenged IRAK-M KO mice showed significantly lower airway reactivity reflected by airway resistance in response to increasing doses of inhaled methacholine than similarly treated-WT mice, n=8 animals in each group, *, $p < 0.05$. (B) Representative photomicrographs of PAS stained-lung tissues showing that OVA-sensitized and -challenged IRAK-M mice had less mucus hypersecretion than the similarly-treated WT mice. Semi-quantitative analysis of PAS scoring using the previously described method, n = 6 animals each group, *, $p < 0.05$. (C) Representative images of Masson Trichrome-stained lung tissue showing less deposit of mature collagen around the airways of IRAK-M KO mice chronically treated with OVA (upper panel). Lung hydroxyproline contents were significantly lower in IRAK-M KO mice chronically treated with OVA than those in similarly challenged-WT mice, n = 3 mice per group from two independent experiments, * $p < 0.05$. (D) Representative image of Western blotting for lung α-SMA expression after chronic OVA induction (upper panel). Semi-quantitative analysis showing significantly lower expression of α-SMA protein in the lungs from IRAK-M KO after chronic OVA induction (lower panel), n =6 mice per group, * $p < 0.05$.

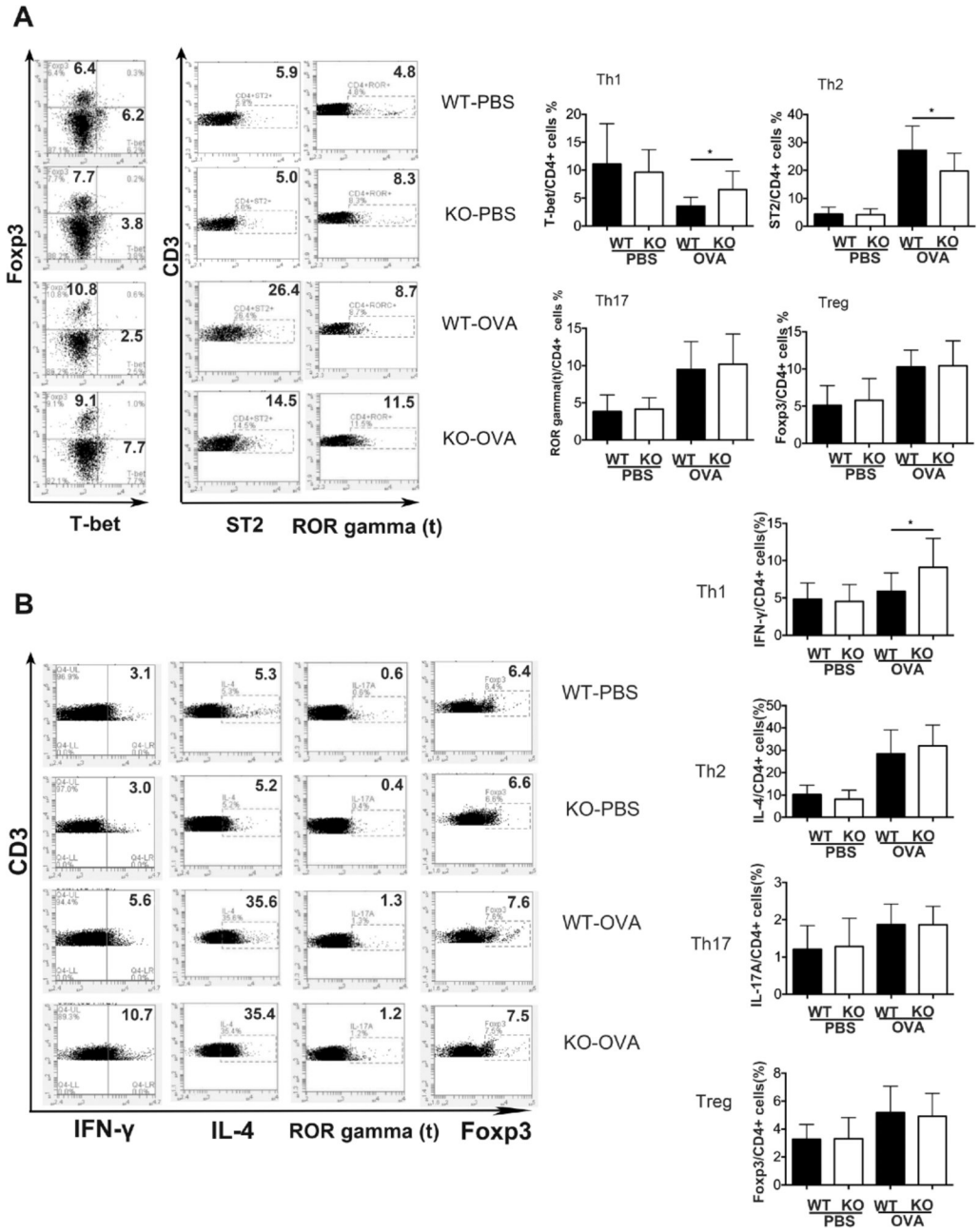

Figure 6. Decreased Th2-mediated immunity in IRAK-M KO mice following chronic OVA stimulation.

Representative image (left panel) and summary plots (right panel) of flowcytometry analysis of Th1, Th2, Th17, and Treg cell percentage in the lungs (A) and spleens (B) of WT or IRAK-M KO mice following chronic PBS or OVA stimulation. n=10 animals in each group, *, $p < 0.05$.

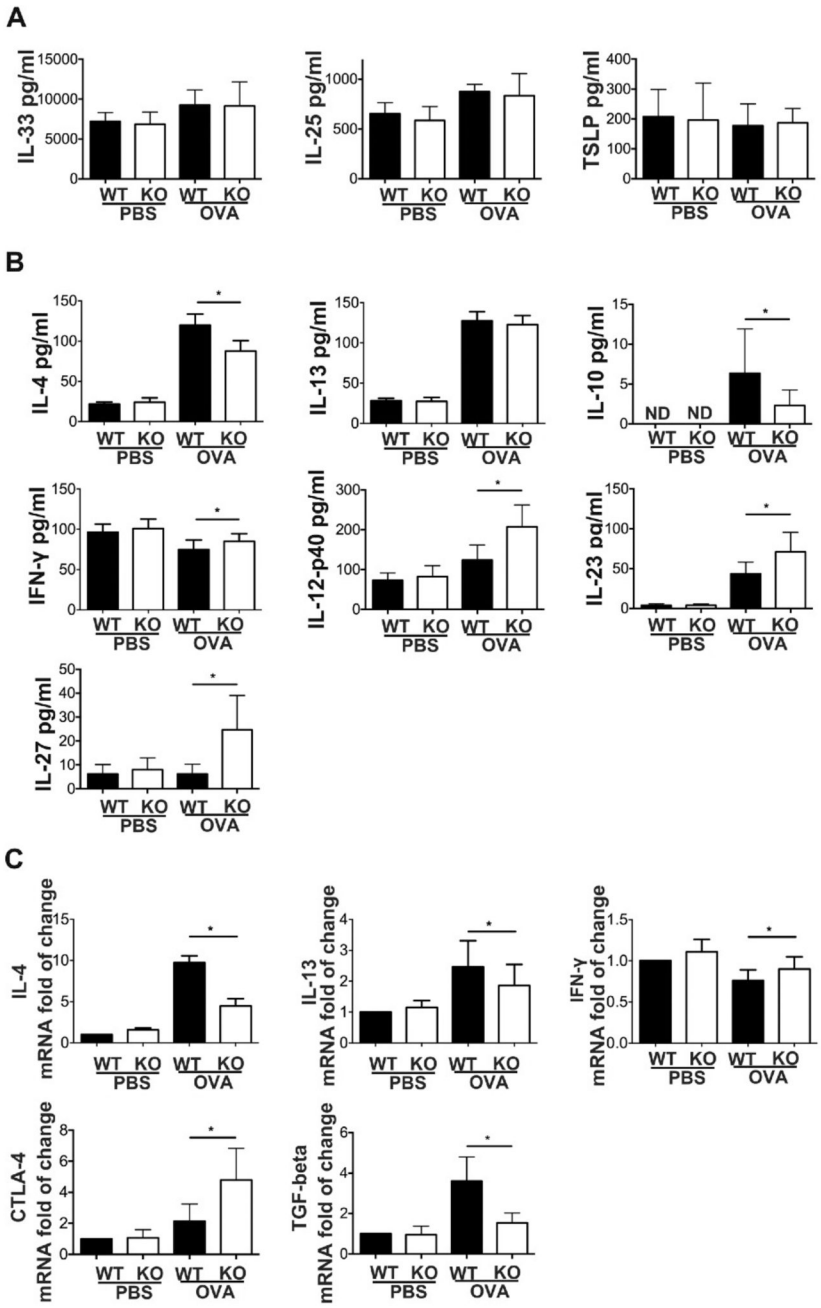

Figure 7. IRAK-M KO influenced on production of Th1/Th2 cytokines in the mouse lungs after chronic OVA induction.

(A) ELISA analysis for levels of epithelial cytokines IL-33, IL-25, and TSLP in the lung homogenates, n=6–8 animals in each group. (B) ELISA analysis for levels of various Th1/Th2 cytokines in BAL fluid from WT or IRAK-M mice following repetitive OVA or PBS stimulation, n=5–8 animals in each group *, $p < 0.05$. (c) qRT-PCR analysis for mRNA expression of IL-4, IL-13, TGF-β1, IFNγ, and CLTA4 in mouse lungs following chronic PBS or OVA treatment, n=6–10 animals in each group, *, $p < 0.05$. TSLP: Thymic strmal lymphopoietin.

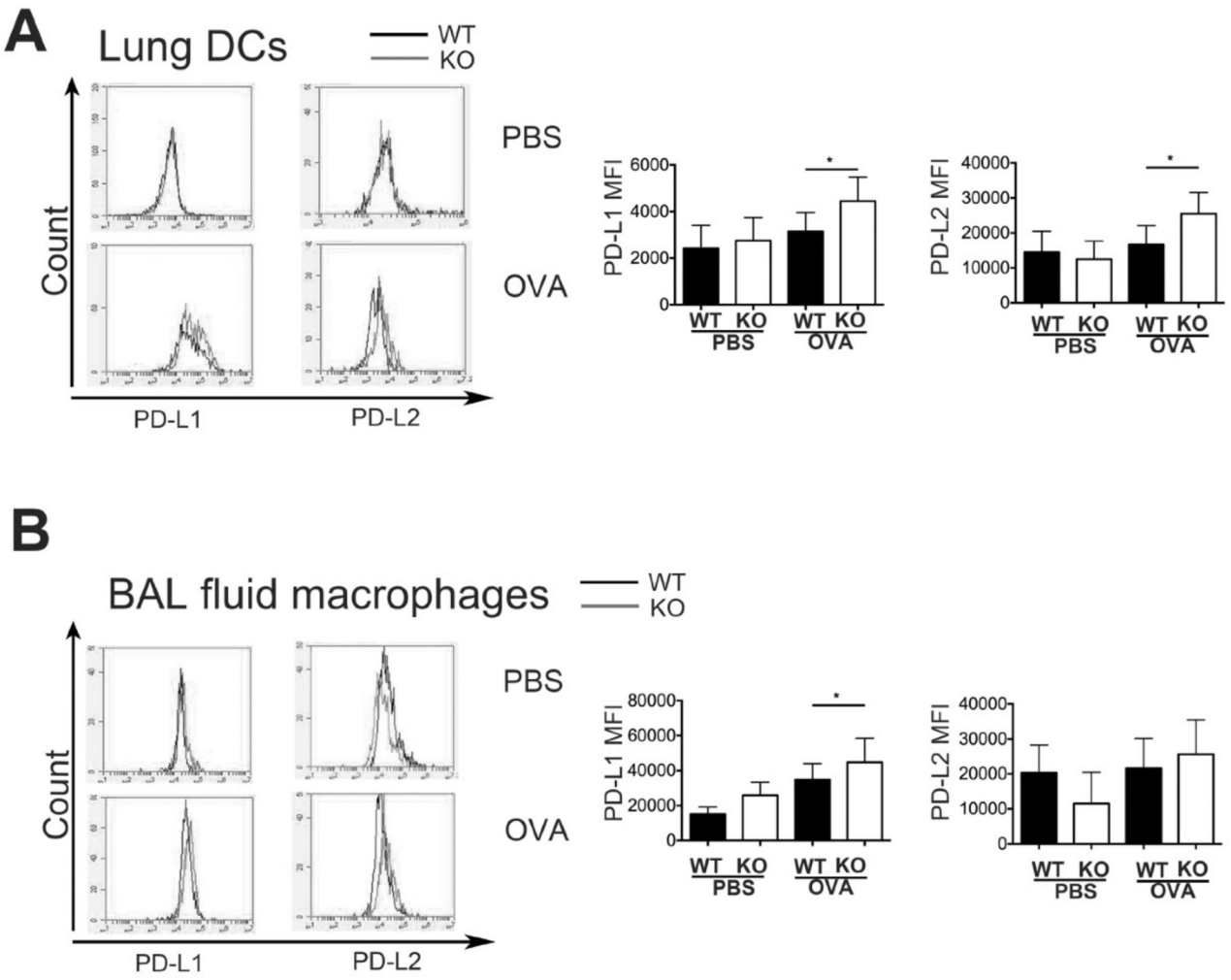

Figure 8. The change induced by IRAK-M KO in the expression of co-stimulatory molecules on DCs and macrophages following a repeated OVA treatment.

Representative images (left panel) and summary plots of flow cytometry analysis of co-stimulatory molecules PD-L1 (CD274) and PD-L2 (CD273) on lung DCs (A) and BAL macrophages (B) from WT or IRAK-M KO mice after chronic OVA or PBS treatment, n=10 animals in each group, *, $p < 0.05$.

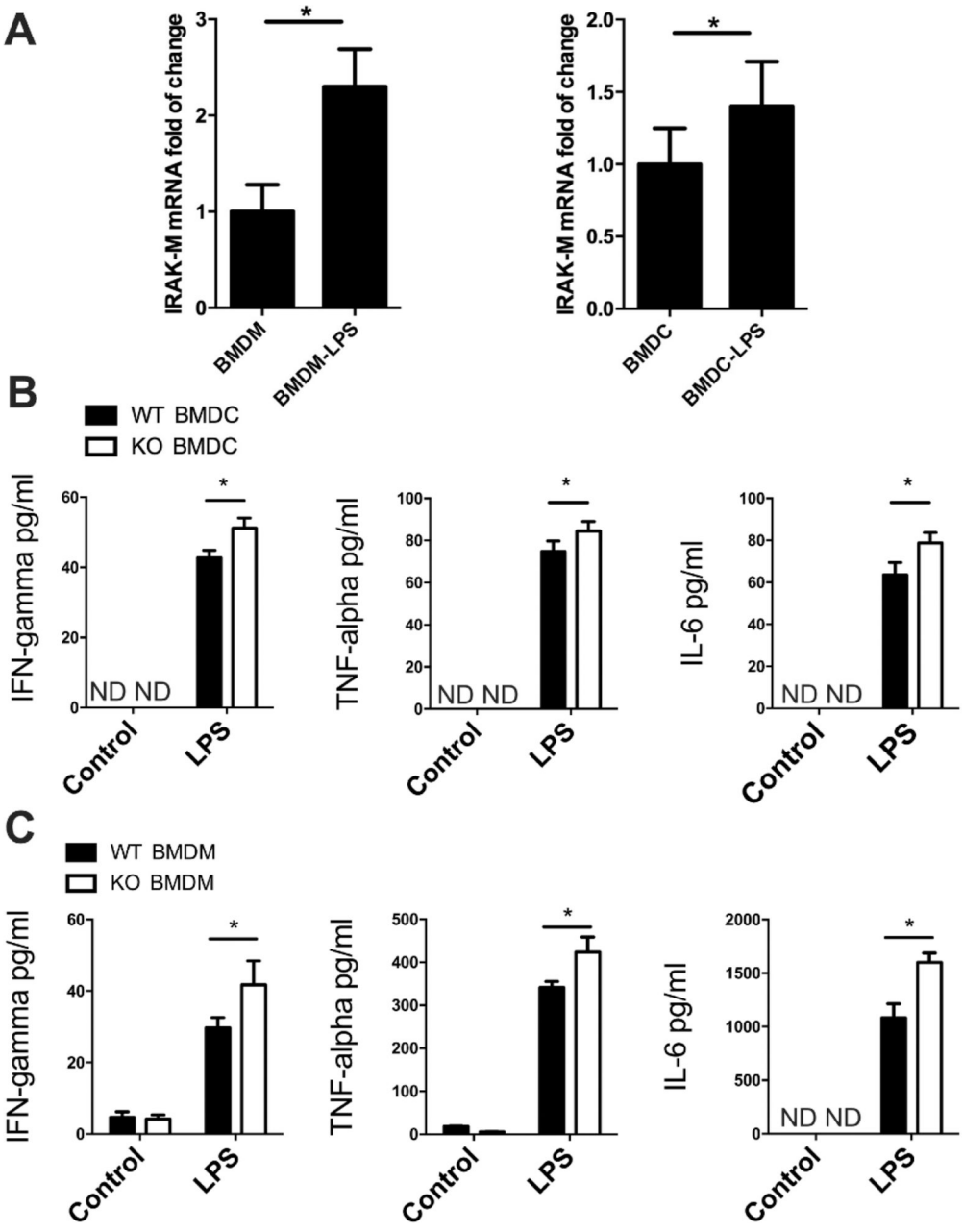

Figure 9. The impact of IRAK-M KO on the Th1 cytokine production by bone marrow-derived dendritic cells (BMDC) and bone marrow-derived macrophages (BMDM).

Expression of IRAK-M mRNA in WT BMDCs and BMDMs stimulated by PBS or LPS, n=10 in each group, *, $p < 0.05$ (A). ELISA analysis of cytokines production by IRAK-M KO or WT BMDCs (B) and BMDMs (C) following in vitro LPS stimulation. n= 6 independent experiments, *, $p < 0.05$.

Table 1

Characteristics of subjects included in this study

Clinical phenotypes	Asthma patients	Controls
Number of subjects	679	669
Mean age (yr)	42.3 ± 14.4	39.4 ± 11.9
Male, no. (%)	285 (41.9)	284 (42.5)
Smoke history (%)	30.8	16.4
Blood Eos (%)	5.6 ± 4.4**	2.3 ± 1.5
Serum LnIgE (U/L)	5.0 ± 1.5**	3.2 ± 1.3
Atopy, n (%)	498 (73.3)	N/A
Allergic rhinitis, n (%)	467 (68.8)	N/A
Lung function parameters		
FEV1 (%)	70.2 ± 23.9#	101.9 ± 12.8
FEV1/FVC (%)	65.2 ± 15.1$	85.4 ± 8.2
Positive for airway challenge test, n (%)	155 (22.8)	N/A
Positive for airway reversibility test, n (%)	524 (77.2)	N/A

N/A: not applicable,

** p<0.01;

# p<0.0001;

$ p<0.001.

FEV1: forced expiratory volume in first second.

FVC: forced vital capacity.

Eos: Eosinophil

Table 2

Distribution of alleles and genotypes of IRAK-M gene in asthma patients and controls

		Alt. frequency		Alt. vs Ref. analysis			Genotype analysis**		
Marker	**Ref./Alt.***	**Case**	**Control**	**P value**	**OR**	**95%CI**	**Case**	**Control**	**P**
rs7970350	T/C	0.227	0.244	0.298	1.100	0.919–1.316	394/231/34	373/264/31	0.240
rs6581660	T/G	0.174	0.166	0.598	0.947	0.774–1.158	454/209/13	459/196/13	0.820
rs11836463	C/A	0.093	0.107	0.204	1.179	0.914–1.520	555/104/10	527/115/13	0.468
rs2870784	G/T	0.085	0.093	0.440	1.110	0.852–1.448	571/99/8	553/107/9	0.742
rs2141709	G/A	0.374	0.389	0.444	1.063	0.909–1.243	270/290/104	253/312/104	0.512
rs2701652	G/C	0.112	0.124	0.338	1.122	0.887–1.419	531/142/5	505/146/9	0.447
rs1821777	C/T	0.110	0.129	0.120	1.203	0.953–1.519	540/129/10	509/147/13	0.300
rs1624395	A/G	0.565	0.514	**0.008**	**1.227**	**1.054–1.428**	127/336/215	152/346/171	**0.025**
rs1370128	T/C	0.550	0.507	**0.027**	**1.187**	**1.020–1.381**	100/407/169	142/375/152	**0.009**

*Ref./Alt.: Reference/Alternative.

**The three values represent the number of individuals carrying major allele homozygote, heterozygote, and mutant allele homozygote.

Bold represents significant value.

Table 3

Association between haplotypes of IRAK-M and asthma

Haplotype	rs2701652	rs1821777	rs1624395	rs1370128	Freq.	Case : Control ratio		Chi square	P value
H1	G	C	G	C	0.394	552.8:803.2,	508.0:830.0	2.209	0.1372
H2	G	C	A	T	0.323	417.2:938.8,	454.0:884.0	3.085	0.079
H3	C	C	G	C	0.109	142.9:1213.1,	149.6:1188.4	0.284	0.594
H4	G	T	A	T	0.105	121.5:1234.5,	162.0:1176.0	0.787	**0.0079**

Bold represents significant value.